

Introduction

In this introductory chapter we describe the *models of one- and two-phase flow problems* that we consider, namely:

- 1) Navier-Stokes equations for one-phase flow (NS1),
- 2) Navier-Stokes equations for two-phase flow (NS2),
- 3) NS2 combined with transport of a dissolved species (NS2+T),
- 4) NS2 combined with transport of a surfactant *on* the interface (NS2+S).

These models are presented in Sect. 1.1 and consist of systems of coupled partial differential equations. To obtain a well-posed problem one has to add appropriate initial- and boundary conditions. This topic is briefly addressed in Sect. 1.2. An illustration of the type of two-phase flows that we are interested in is given in Sect. 1.3, where we present results of some numerical simulations. In Sect. 1.4 we give a schematic overview of the numerical methods that will be treated.

1.1 One- and two-phase flow models in strong formulation

In this section we give the partial differential equations corresponding to the models 1)-4). For ease of presentation these partial differential equations are given in the *strong* formulation. The numerical methods, in particular the finite element methods for spatial discretization, are based on the *weak* formulation of these partial differential equations. These weak formulations are given further on. In Sect. 1.2 we address the issue of initial and boundary conditions used in our models.

We always assume that the physical domain $\Omega \subset \mathbb{R}^3$ is an open bounded domain. This domain will also be the computational domain. We consider the flow problems for a fixed time interval denoted by $[0, T]$.

1.1.1 Navier-Stokes equations for one-phase flow

We derive the Navier-Stokes equations for modeling a laminar fluid flow. We assume the fluid to be incompressible, viscous, Newtonian and pure (i.e., no mixture of different components). Moreover we assume isothermal conditions and therefore neglect variations of density and dynamic viscosity due to temperature changes. Hence, dynamic viscosity and, due to incompressibility, also the density are constant (and positive).

The Eulerian coordinates of a point in Ω are denoted by $x = (x_1, x_2, x_3)$. We take a fixed $t_0 \in (0, T)$ and consider a time interval $(t_0 - \delta, t_0 + \delta)$, with $\delta > 0$ sufficiently small such that for $t \in (t_0 - \delta, t_0 + \delta)$ the quantities introduced below are well-defined. Let \mathbf{X} denote a particle (also called “material point”) in Ω at $t = t_0$, with Eulerian coordinates $\xi \in \mathbb{R}^3$. Let $X_\xi(t)$ denote the Eulerian coordinates of the particle \mathbf{X} at time t . The mapping

$$t \rightarrow X_\xi(t), \quad t \in (t_0 - \delta, t_0 + \delta),$$

describes the trajectory of the particle \mathbf{X} . The particles are transported by a velocity field, which is denoted by $\mathbf{u} = \mathbf{u}(x, t) = (u_1(x, t), u_2(x, t), u_3(x, t)) \in \mathbb{R}^3$. Hence

$$\frac{d}{dt}X_\xi(t) = \mathbf{u}(X_\xi(t), t). \quad (1.1)$$

For the given \mathbf{X} , the solution of the system of ordinary differential equations

$$\frac{d}{dt}X_\xi(t) = \mathbf{u}(X_\xi(t), t), \quad t \in (t_0 - \delta, t_0 + \delta), \quad X_\xi(t_0) = \xi,$$

yields the trajectory of the particle \mathbf{X} .

Physical processes can be modeled in different coordinate systems. For flow problems, the two most important ones are (x, t) (“Eulerian”) and (ξ, t) (“Lagrangian”):

- Euler coordinates (x, t) : one takes an arbitrary fixed point x in space and considers the velocity $\mathbf{u}(x, t)$ at x . If time evolves *different* particles pass through x .
- Lagrange (or “material”) coordinates (ξ, t) : one takes an arbitrary fixed particle (material point) and considers its motion. If time evolves one thus follows the trajectory of a *fixed* particle.

Related to the Lagrangian coordinates we define the so-called *material derivative* of a (sufficiently smooth) function $f(x, t)$ on the trajectory of \mathbf{X} :

$$\dot{f}(X_\xi(t), t) := \frac{d}{dt}f(X_\xi(t), t).$$

If f is defined in a neighborhood of the trajectory we obtain from the chain rule and (1.1):

$$\dot{f} = \frac{\partial f}{\partial t} + \mathbf{u} \cdot \nabla f. \quad (1.2)$$

The derivation of partial differential equations that model the flow problem is based on conservation laws applied on a (small) subdomain, called a material volume, $W_0 \subset \Omega$. We derive these partial differential equations in Eulerian coordinates. Given W_0 , define

$$W(t) := \{ X_\xi(t) : \xi \in W_0 \}.$$

$W(t)$ describes the position of the particles at time t , which were located in W_0 at time $t = t_0$. We need the following fundamental identity, which holds for a scalar sufficiently smooth function $f = f(x, t)$:

Reynolds' transport theorem:

$$\begin{aligned} \frac{d}{dt} \int_{W(t)} f(x, t) dx &= \int_{W(t)} \dot{f}(x, t) + f \operatorname{div} \mathbf{u}(x, t) dx \\ &= \int_{W(t)} \frac{\partial f}{\partial t}(x, t) + \operatorname{div}(f \mathbf{u})(x, t) dx, \end{aligned} \quad (1.3)$$

with $\dot{f} := \frac{\partial f}{\partial t} + \mathbf{u} \cdot \nabla f$ the material derivative.

First we consider the *conservation of mass* principle. Let $\rho(x, t)$ be the *density* of the fluid. If we take $f = \rho$ in (1.3) this yields

$$0 = \frac{d}{dt} \int_{W(t)} \rho dx = \int_{W(t)} \frac{\partial \rho}{\partial t} + \operatorname{div}(\rho \mathbf{u}) dx,$$

which holds in particular for $t = t_0$ and for an arbitrary material volume $W(t_0) = W_0$ in Ω . Since also $t_0 \in (0, T)$ is arbitrary, we obtain the partial differential equation

$$\frac{\partial \rho}{\partial t} + \operatorname{div}(\rho \mathbf{u}) = 0 \quad \text{in } \Omega \times (0, T).$$

Due to the assumption $\rho = \text{const}$ this simplifies to

$$\operatorname{div} \mathbf{u} = 0 \quad \text{in } \Omega \times (0, T), \quad (1.4)$$

which is often called *mass conservation equation* or *continuity equation*.

We now consider *conservation of momentum*. The momentum of mass contained in $W(t)$ is given by

$$M(t) = \int_{W(t)} \rho \mathbf{u} dx.$$

Due to Newton's law the *change* of momentum $M(t)$ is equal to the force $F(t)$ acting on $W(t)$. This force is decomposed in a *volume* force $F_1(t)$ and a

boundary force $F_2(t)$. We restrict ourselves to the case where the only volume force acting on the volume $W(t)$ is gravity:

$$F_1(t) = \int_{W(t)} \rho \mathbf{g} \, dx,$$

where $\mathbf{g} \in \mathbb{R}^3$ is the vector of gravitational acceleration. The boundary force $F_2(t)$ is used to describe internal forces, i.e., forces that a fluid exerts on itself. These include pressure and the viscous drag that a fluid element $W(t)$ gets from the adjacent fluid. These internal forces are *contact* forces: they act on the boundary $\partial W(t)$ of the fluid element $W(t)$. Let \vec{t} denote this internal force vector, also called traction vector. Then we have

$$F_2(t) = \int_{\partial W(t)} \vec{t} \, ds.$$

Cauchy derived fundamental principles of continuum mechanics and in particular he derived the following law (often called *Cauchy's theorem*):

\vec{t} is a linear function of \mathbf{n} ,

where $\mathbf{n} = \mathbf{n}(x, t) \in \mathbb{R}^3$ is the outer unit normal on $\partial W(t)$. For more explanation on this we refer to introductions to continuum mechanics, for example [130]. Thus it follows that there is a matrix $\boldsymbol{\sigma} = \boldsymbol{\sigma}(x, t) \in \mathbb{R}^{3 \times 3}$, called the *stress tensor*, such that the boundary force can be represented as

$$F_2(t) = \int_{\partial W(t)} \boldsymbol{\sigma} \mathbf{n} \, ds. \quad (1.5)$$

Using these force representations in Newton's law and applying Stokes' theorem for $F_2(t)$ we get

$$\begin{aligned} \frac{d}{dt} M(t) &= F_1(t) + F_2(t) \\ &= \int_{W(t)} \rho \mathbf{g} + \operatorname{div} \boldsymbol{\sigma} \, dx. \end{aligned} \quad (1.6)$$

For a matrix $\mathbf{A}(x) \in \mathbb{R}^3$, $x \in \mathbb{R}^3$, its divergence is defined by

$$\operatorname{div} \mathbf{A}(x) = \begin{pmatrix} \operatorname{div}(a_{11} & a_{12} & a_{13}) \\ \operatorname{div}(a_{21} & a_{22} & a_{23}) \\ \operatorname{div}(a_{31} & a_{32} & a_{33}) \end{pmatrix} \in \mathbb{R}^3.$$

Using the transport theorem (1.3) in the left-hand side of (1.6) with $f = \rho u_i$, $i = 1, 2, 3$, we obtain

$$\int_{W(t)} \frac{\partial \rho u_i}{\partial t} + \operatorname{div}(\rho u_i \mathbf{u}) \, dx = \int_{W(t)} \rho g_i + \operatorname{div} \boldsymbol{\sigma}_i \, dx, \quad i = 1, 2, 3,$$

with σ_i the i -th row of σ and g_i the i -th component of \mathbf{g} . In vector notation, with $\mathbf{u} \otimes \mathbf{u} = (u_i u_j)_{1 \leq i, j \leq 3}$,

$$\int_{W(t)} \frac{\partial \rho \mathbf{u}}{\partial t} + \operatorname{div}(\rho \mathbf{u} \otimes \mathbf{u}) \, dx = \int_{W(t)} \rho \mathbf{g} + \operatorname{div} \sigma \, dx, \quad (1.7)$$

which holds in particular for $t = t_0$ and for an arbitrary material volume $W(t_0) = W_0$ in Ω . Since $t_0 \in (0, T)$ is arbitrary, we obtain the partial differential equations

$$\frac{\partial \rho \mathbf{u}}{\partial t} + \operatorname{div}(\rho \mathbf{u} \otimes \mathbf{u}) = \rho \mathbf{g} + \operatorname{div} \sigma \quad \text{in } \Omega \times (0, T).$$

Note that $\operatorname{div}(\rho \mathbf{u} \otimes \mathbf{u}) = \rho(\mathbf{u} \cdot \nabla) \mathbf{u} + \rho \mathbf{u} \operatorname{div} \mathbf{u}$ and due to the continuity equation (1.4), the last summand vanishes, yielding the so-called *momentum equation*

$$\rho \frac{\partial \mathbf{u}}{\partial t} + \rho(\mathbf{u} \cdot \nabla) \mathbf{u} = \rho \mathbf{g} + \operatorname{div} \sigma. \quad (1.8)$$

For viscous *Newtonian fluids* one assumes that the stress tensor σ is of the form

$$\sigma = -p\mathbf{I} + L(\mathbf{D}), \quad (1.9)$$

where p is the pressure,

$$\mathbf{D}(\mathbf{u}) = \nabla \mathbf{u} + (\nabla \mathbf{u})^T$$

is the deformation tensor, $\nabla \mathbf{u} := (\nabla u_1 \, \nabla u_2 \, \nabla u_3)$, and L is assumed to be a *linear* mapping. Based on this structural model for the stress tensor and using the additional assumptions that the medium is isotropic (i.e. its properties are the same in all space directions) and the action of the stress tensor is independent of the specific frame of reference (“invariance under a change in observer”) it can be shown ([130, 107]) that the stress tensor must have the form

$$\sigma = -p\mathbf{I} + \lambda \operatorname{div} \mathbf{u} \mathbf{I} + \mu \mathbf{D}(\mathbf{u}). \quad (1.10)$$

Further physical considerations lead to relations for the parameters μ , λ , e.g., $\mu > 0$ (for a viscous fluid), $\lambda \geq -\frac{2}{3}\mu$ or even $\lambda = -\frac{2}{3}\mu$. For the case of an incompressible fluid, i.e., $\operatorname{div} \mathbf{u} = 0$, the relation for the stress tensor simplifies to

$$\sigma = -p\mathbf{I} + \mu \mathbf{D}(\mathbf{u}), \quad (1.11)$$

with $\mu > 0$ the *dynamic viscosity*. Hence, we obtain the fundamental Navier-Stokes equations for incompressible flow:

$$\begin{aligned} \rho \left(\frac{\partial \mathbf{u}}{\partial t} + (\mathbf{u} \cdot \nabla) \mathbf{u} \right) &= -\nabla p + \operatorname{div}(\mu \mathbf{D}(\mathbf{u})) + \rho \mathbf{g} \quad \text{in } \Omega \\ \operatorname{div} \mathbf{u} &= 0 \quad \text{in } \Omega. \end{aligned} \quad (1.12)$$

These equations are considered for $t \in [0, T]$. Initial and boundary conditions corresponding to these Navier-Stokes equations are discussed in Sect. 1.2.

Remark 1.1.1 Using the assumption that μ is a strictly positive *constant* and the relation $\operatorname{div} \mathbf{u} = 0$ we get

$$\operatorname{div}(\mu \mathbf{D}(\mathbf{u})) = \mu \Delta \mathbf{u} = \mu \begin{pmatrix} \Delta u_1 \\ \Delta u_2 \\ \Delta u_3 \end{pmatrix}.$$

1.1.2 Navier-Stokes equations for two-phase flow

We now consider two-phase flows, i.e., Ω contains two different *immiscible* incompressible phases (liquid-liquid or liquid-gas) which may move in time and have different material properties ρ_i and μ_i , $i = 1, 2$. For each point in time, $t \in [0, T]$, Ω is partitioned into two open subdomains $\Omega_1(t)$ and $\Omega_2(t)$, $\overline{\Omega} = \overline{\Omega}_1(t) \cup \overline{\Omega}_2(t)$, $\Omega_1(t) \cap \Omega_2(t) = \emptyset$, each of them containing one of the phases, respectively. These phases are separated from each other by the interface $\Gamma(t) = \overline{\Omega}_1(t) \cap \overline{\Omega}_2(t)$, cf. Fig. 1.1. As mentioned before, we assume isothermal conditions and both phases to be pure substances. Furthermore, we do *not* consider reaction, mass transfer or phase transition.

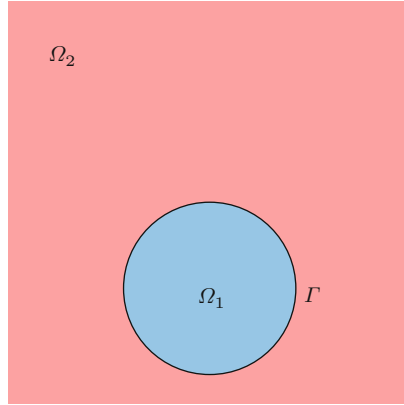


Fig. 1.1. 2D illustration of a domain Ω consisting of two phases Ω_1 and Ω_2 and interface Γ .

In each of the phases conservation of mass and momentum has to hold, yielding separate Navier-Stokes equations in the two domains Ω_i , $i = 1, 2$:

$$\begin{cases} \rho_i \left(\frac{\partial \mathbf{u}}{\partial t} + (\mathbf{u} \cdot \nabla) \mathbf{u} \right) = \operatorname{div} \boldsymbol{\sigma}_i + \rho_i \mathbf{g} & \text{in } \Omega_i, \ i = 1, 2, \\ \operatorname{div} \mathbf{u} = 0 \end{cases} \quad (1.13)$$

with $\sigma_i = -p\mathbf{I} + \mu_i(\nabla \mathbf{u} + (\nabla \mathbf{u})^T)$. We now derive *coupling conditions* at the interface. As the phases are viscous and no phase transition takes place, the velocity can be assumed to be continuous at the interface:

$$[\mathbf{u}] = 0 \quad \text{on } \Gamma. \quad (1.14)$$

Here for $x \in \Gamma$ and a function f defined in a neighborhood of Γ we define the jump across Γ by

$$[f](x) = [f]_\Gamma(x) := \lim_{h \downarrow 0} (f(x - h \mathbf{n}_\Gamma(x)) - f(x + h \mathbf{n}_\Gamma(x))), \quad (1.15)$$

where $\mathbf{n}_\Gamma(x)$ denotes the unit normal on Γ at x , pointing from Ω_1 to Ω_2 .

Remark 1.1.2 In the definition of the jump across the interface in (1.15) the normal is pointing from Ω_1 into Ω_2 and the jump is defined as the value close to the interface in Ω_1 minus the value close to the interface in Ω_2 . In the literature sometimes the other sign convention (value in Ω_2 minus value in Ω_1) is used, leading to another sign in the interface condition (1.19) derived below. We choose this sign convention, since it is consistent with the standard form of the classical Laplace-Young pressure jump relation $[p]_\Gamma = \tau \kappa \mathbf{n}$, discussed in Remark 1.1.5.

Consider a fluid volume $W = W_1 \cup W_2$ as illustrated in Fig. 1.2 which contains a part γ of the interface Γ .

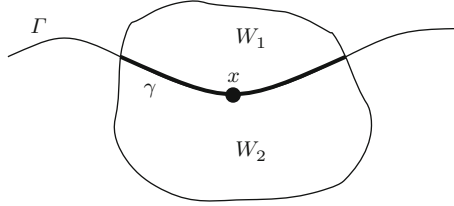


Fig. 1.2. 2D illustration of a neighborhood $W = W_1 \cup W_2$ for an interface point $x \in \Gamma$.

At the interface acts a *surface tension force* which is due to the fact that on both sides of Γ there are different molecules that have different attractive forces. The surface tension force acting on the interface segment γ can be modeled by (cf. [225, 47, 219] and Sect. 1.1.5)

$$F_3(t) = -\tau \int_{\gamma(t)} \kappa \mathbf{n}_\Gamma ds. \quad (1.16)$$

The parameter τ is the *surface tension coefficient*, which is a material property of the two-phase system. To simplify the presentation we assume τ to be constant. For many two-phase systems this is a reasonable assumption. The

case of a variable surface tension coefficient τ is discussed in Remark 1.1.3. The scalar function $\kappa(x)$, $x \in \Gamma$, is the mean curvature, cf. Chap. 14, for which

$$\kappa(x) = \operatorname{div} \mathbf{n}_\Gamma(x), \quad x \in \Gamma,$$

holds. Note that if at $x \in \Gamma$ the subdomain Ω_1 is locally convex, then κ is positive. This additional force term $F_3(t)$ has to be taken into account if we consider conservation of momentum, cf. Sect. 1.1.1. For a fluid volume $W = W_1 \cup W_2$ as in Fig. 1.2, instead of (1.5), (1.6) we now have

$$\begin{aligned} \frac{d}{dt} M(t) &= F_1(t) + F_2(t) + F_3(t) \\ &= \int_{W(t)} \rho \mathbf{g} \, dx + \int_{\partial W(t)} \boldsymbol{\sigma} \mathbf{n} \, ds - \tau \int_{\gamma(t)} \kappa \mathbf{n}_\Gamma \, ds. \end{aligned} \quad (1.17)$$

Since the stress tensor $\boldsymbol{\sigma}$ is not necessarily smooth across Γ we split ∂W into ∂W_1 and ∂W_2

$$\int_{\partial W(t)} \boldsymbol{\sigma} \mathbf{n} \, ds = \int_{\partial W_1(t)} \boldsymbol{\sigma}_1 \mathbf{n}_1 \, ds + \int_{\partial W_2(t)} \boldsymbol{\sigma}_2 \mathbf{n}_2 \, ds - \int_{\gamma(t)} [\boldsymbol{\sigma}] \mathbf{n}_\Gamma \, ds,$$

and apply the Stokes' theorem on W_1 and W_2 separately. Note that \mathbf{n}_i is the outward normal on ∂W_i and \mathbf{n}_Γ the normal at Γ , pointing from Ω_1 in Ω_2 . Thus we obtain, cf. (1.7),

$$\begin{aligned} \int_{W(t)} \rho \left(\frac{\partial \mathbf{u}}{\partial t} + (\mathbf{u} \cdot \nabla) \cdot \mathbf{u} \right) dx &= \int_{W_1(t)} \operatorname{div} \boldsymbol{\sigma}_1 \, dx + \int_{W_2(t)} \operatorname{div} \boldsymbol{\sigma}_2 \, dx \\ &\quad + \int_{W(t)} \rho \mathbf{g} \, dx - \int_{\gamma(t)} [\boldsymbol{\sigma}] \mathbf{n}_\Gamma \, ds - \tau \int_{\gamma(t)} \kappa \mathbf{n}_\Gamma \, ds. \end{aligned}$$

This yields,

$$\sum_{i=1,2} \int_{W_i(t)} \rho_i \left(\frac{\partial \mathbf{u}}{\partial t} + (\mathbf{u} \cdot \nabla) \cdot \mathbf{u} \right) - \operatorname{div} \boldsymbol{\sigma}_i - \rho_i \mathbf{g} \, dx = - \int_{\gamma(t)} \tau \kappa \mathbf{n}_\Gamma + [\boldsymbol{\sigma}] \mathbf{n}_\Gamma \, ds.$$

Due to momentum conservation in W_i , $i = 1, 2$, the left-hand side equals zero, cf. (1.13). Since $W(t)$ can be varied we thus obtain the coupling condition:

$$[\boldsymbol{\sigma} \mathbf{n}_\Gamma] = [\boldsymbol{\sigma}] \mathbf{n}_\Gamma = -\tau \kappa \mathbf{n}_\Gamma \quad \text{on } \Gamma. \quad (1.18)$$

Finally, in view of the immiscibility assumption we introduce the normal velocity $V_\Gamma = V_\Gamma(x, t) \in \mathbb{R}$, which denotes the *size* of the velocity of the interface Γ at $x \in \Gamma(t)$ in normal direction, i.e., the movement of Γ in normal direction is given by $V_\Gamma \mathbf{n}$. The *immiscibility assumption* is modeled by the condition that the normal velocity of the interface should equal the normal component of the flow field at the interface, i.e. $V_\Gamma = \mathbf{u} \cdot \mathbf{n}_\Gamma$ at the interface. Summarizing, the latter condition, the equations in (1.13) and the coupling conditions in (1.14) and (1.18) lead to the following standard model for two-phase flows:

$$\begin{cases} \rho_i \left(\frac{\partial \mathbf{u}}{\partial t} + (\mathbf{u} \cdot \nabla) \mathbf{u} \right) = \operatorname{div} \boldsymbol{\sigma}_i + \rho_i \mathbf{g} & \text{in } \Omega_i, \quad i = 1, 2, \\ \operatorname{div} \mathbf{u} = 0 \end{cases} \quad (1.19)$$

$$[\boldsymbol{\sigma} \mathbf{n}_\Gamma] = -\tau \kappa \mathbf{n}_\Gamma, \quad [\mathbf{u}] = 0 \quad \text{on } \Gamma, \quad (1.20)$$

$$V_\Gamma = \mathbf{u} \cdot \mathbf{n}_\Gamma \quad \text{on } \Gamma. \quad (1.21)$$

We recall the Newtonian stress tensor model: $\boldsymbol{\sigma}_i = -p\mathbf{I} + \mu_i(\nabla \mathbf{u} + (\nabla \mathbf{u})^T)$. The density and viscosity, ρ_i and μ_i , $i = 1, 2$, are assumed to be constant in each phase.

Remark 1.1.3 In certain cases, for example in systems with significant surfactants (“surface active agents”) one has to take a *variable* surface tension coefficient τ into account, cf. Sect. 1.1.5. In that case the surface tension force in (1.16) has to be replaced by its generalization

$$F_3(t) = - \int_\gamma \tau \kappa \mathbf{n}_\Gamma - \nabla_\Gamma \tau \, ds, \quad (1.22)$$

where $\nabla_\Gamma = P\nabla$, with $P = I - \mathbf{n}_\Gamma \mathbf{n}_\Gamma^T$, is the *tangential derivative*. The interface condition in (1.18) then generalizes to

$$[\boldsymbol{\sigma} \mathbf{n}_\Gamma] = -\tau \kappa \mathbf{n}_\Gamma + \nabla_\Gamma \tau. \quad (1.23)$$

In the remainder we often write \mathbf{n} instead of \mathbf{n}_Γ .

1.1.3 Two-phase flow with transport of a dissolved species

We consider a two-phase flow problem as described above. We assume that one or both phases contain a dissolved species that is transported due to convection and molecular diffusion and does not adhere to the interface. The concentration of this species is denoted by $c(x, t)$. This flow problem can be modeled by the equations (1.19)-(1.21) for the flow variables and a convection-diffusion equation for the concentration c . At the interface we need interface conditions for c . The first interface condition comes from mass conservation, which implies flux continuity. The second condition results from a constitutive equation known as Henry’s law, which states that the solubility of a gas in a liquid at a particular temperature is proportional to the pressure of that gas above the liquid. In mathematical terms this relation (at constant temperature) can be formulated as $p = k_H c$ where p is the partial pressure of the solute in the gas above the solution, c is the concentration of the solute and k_H is known as the Henry’s law constant and depends on the solute, the solvent and the temperature. The same solute in different solvents (at the same temperature) corresponds to different Henry constants, reflecting the different

solubility properties of the two solvents. From this it can be deduced, that in a two-phase system with a solute, assuming instantaneous local equilibrium at the interface, there is a constant ratio between the concentrations of the solute on the two sides of the interface. Thus one obtains the following standard model:

Two-phase flow model (1.19) – (1.21) combined with:

$$\begin{aligned} \frac{\partial c}{\partial t} + \mathbf{u} \cdot \nabla c &= \operatorname{div}(D_i \nabla c) \quad \text{in } \Omega_i, \quad i = 1, 2, \\ [D_i \nabla c \cdot \mathbf{n}]_F &= 0 \quad \text{on } F, \\ c_1 &= C_H c_2 \quad \text{on } F. \end{aligned} \tag{1.24}$$

The diffusion coefficient D_i is piecewise constant. In the interface condition we use the notation c_i for $c|_{\Omega_i}$ restricted to the interface. The constant $C_H > 0$ is given (Henry's constant). The Henry interface condition can also be written as $[\hat{C}c] = 0$, with $\hat{C} = 1$ in Ω_1 , $\hat{C} = C_H$ in Ω_2 . The model has to be combined with suitable initial and boundary conditions, cf. Sect. 1.2. In the formulation in (1.24) there is a coupling between fluid dynamics and mass transport only *in one direction*, in the sense that the velocity is used in the mass transport equation, but the concentration c does *not* influence the fluid dynamics. In certain systems it may be appropriate to consider a dependence of the surface tension coefficient on c , i.e. $\tau = \tau(c)$. In that case there is a coupling in two directions between fluid dynamics and mass transport.

1.1.4 Two-phase flow with transport of a surfactant on the interface

We consider a two-phase flow problem as described above in Sect. 1.1.2. We assume that there is a species (called tenside or surfactant) which adheres to the interface and is transported at the interface due to convection (movement of the interface) and due to diffusion (molecular diffusion on the interface). For simplicity we assume that there are no adsorption and desorption effects (i.e. no sources or sinks). The concentration of this surfactant is denoted by $S(x, t)$, $x \in \Gamma(t)$. A partial differential equation for this quantity can be derived from the conservation of mass principle (on subsets $\gamma(t)$ of the moving interface $\Gamma(t)$). For $t_0 \in (0, T)$, let γ_0 be a connected bounded subset of $\Gamma(t_0)$ and $\gamma(t) = \{X_\xi(t) : \xi \in \gamma_0\} \subset \Gamma(t)$, $t \in (t_0 - \delta, t_0 + \delta)$, with $\delta > 0$ sufficiently small. The conservation of mass property yields

$$\frac{d}{dt} \int_{\gamma(t)} S \, ds = - \int_{\partial\gamma(t)} q \cdot n \, d\tilde{s},$$

with n the unit normal to $\partial\gamma(t)$ lying in a tangent plane and pointing out of $\gamma(t)$.

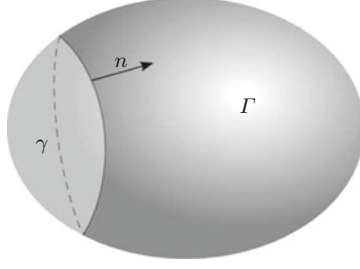


Fig. 1.3. Interface Γ and subset $\gamma \subset \Gamma$, with vector n which is normal to $\partial\gamma$ and tangential to Γ .

We restrict to the case of a *diffusive flux* $q := -D_\Gamma \nabla_\Gamma S$. Recall that the tangential derivative is defined by $\nabla_\Gamma := \mathbf{P} \nabla$ with $\mathbf{P} = \mathbf{I} - \mathbf{n} \mathbf{n}^T$. Note that the normal $\mathbf{n} = \mathbf{n}_\Gamma$ differs from the normal n . Using integration by parts on the manifold $\gamma(t)$ we obtain

$$\int_{\partial\gamma(t)} q \cdot n \, d\tilde{s} = \int_{\gamma(t)} \operatorname{div}_\Gamma q \, ds.$$

A variant of the transport theorem in (1.3), cf. (14.21b) and Remark 14.2.3, yields

$$\frac{d}{dt} \int_{\gamma(t)} S \, ds = \int_{\gamma(t)} \dot{S} + S \operatorname{div}_\Gamma \mathbf{u} \, ds$$

and thus we obtain

$$\int_{\gamma(t)} \dot{S} + S \operatorname{div}_\Gamma \mathbf{u} + \operatorname{div}_\Gamma q \, ds = 0,$$

which holds in particular for $\gamma(t_0) = \gamma_0$ arbitrary. Hence we obtain the following model for transport of surfactants:

Two-phase flow model (1.19) – (1.21) combined with:

$$\dot{S} + S \operatorname{div}_\Gamma \mathbf{u} = \operatorname{div}_\Gamma (D_\Gamma \nabla_\Gamma S) \quad \text{on } \Gamma. \quad (1.25)$$

If the diffusion coefficient D_Γ is constant on Γ we can reformulate the diffusion part as $\operatorname{div}_\Gamma (D_\Gamma \nabla_\Gamma S) = D_\Gamma \Delta_\Gamma S$. Using the definition of the material derivative the convection-diffusion equation in (1.25) can be written as

$$\frac{\partial S}{\partial t} + \mathbf{u} \cdot \nabla S + S \operatorname{div}_\Gamma \mathbf{u} = D_\Gamma \Delta_\Gamma S \quad \text{on } \Gamma.$$

In this formulation, for the partial derivatives $\frac{\partial}{\partial t}$ and $\mathbf{u} \cdot \nabla$ to be well-defined, one assumes that S is smoothly extended in a small neighborhood of Γ . For

this surfactant transport equation no boundary conditions are needed if the interface Γ is a surface without boundary. In case of a stationary interface, i.e. $\mathbf{u} \cdot \mathbf{n} = 0$ on Γ , we have $\mathbf{P}\mathbf{u} = \mathbf{u}$ and thus $\mathbf{u} \cdot \nabla S + S \operatorname{div}_\Gamma \mathbf{u} = \mathbf{u} \cdot \nabla_\Gamma S + S \operatorname{div}_\Gamma \mathbf{u} = \operatorname{div}_\Gamma(\mathbf{u}S)$. Hence, we obtain the (simplified) diffusion equation $\frac{\partial S}{\partial t} + \operatorname{div}_\Gamma(\mathbf{u}S) - D_\Gamma \Delta_\Gamma S = 0$.

In the formulation in (1.25) there is a coupling between fluid dynamics and surfactant transport only *in one direction*, in the sense that the velocity is used in the surfactant transport equation, but the surfactant concentration S does *not* influence the fluid dynamics. In many systems with surfactants, there is a dependence of the surface tension coefficient on S , i.e. $\tau = \tau(S)$. In that case there is a coupling in two directions between fluid dynamics and surfactant transport.

1.1.5 Modeling of interfacial phenomena

The notion of interfacial transport phenomena usually refers to mass, momentum and energy transfer within a neighborhood of an interface, including the thermodynamics of the interface. Physico-chemical interfacial phenomena play a crucial role in high-tech applications like, for example, lab-on-a-chip systems, multiphase reactors in chemical engineering and micro process engineering. We refer to the (chemical) engineering literature for a treatment of these topics, e.g. [40], in which particle-stabilized foams and emulsions and new materials derived from such systems are studied. The understanding of most of these interfacial phenomena is still very poor. In particular there is a strong lack of (validated) mathematical models that describe interfacial processes appropriately. Research on modeling of interfacial transport phenomena is a very active and rapidly growing field. We do not treat modeling aspects in this monograph. In this section we only give a very brief introduction into basics related to the modeling of interfacial processes in two-phase incompressible immiscible flows. An extensive treatment of this topic and many references are given in [225].

Dividing surface and clean interface

There are continuum models in which an interface is represented as a *three-dimensional* region of very small thickness. One of the first models of this type was introduced by Korteweg [158]. The so-called phase field (or diffusive interface) models, treated in Sect. 6.2.4, belong to this class. More often models are used in which the interface is modeled by a (non-physical) *two-dimensional dividing surface*. This approach was first proposed by Gibbs. In such a *sharp interface model* for incompressible flows it is assumed that the dividing surface separates two homogeneous phases which both have a constant density. The effect of the interfacial region is taken into account by introducing so-called *excess* quantities (e.g., mass and energy) which are assigned to the

dividing surface. We explain this by considering the excess mass density, denoted by ρ^Γ . For a given time t let $W(t)$ be a material volume, illustrated in Fig. 1.4, which contains two phases and an interfacial region of finite thickness. This interfacial region, denoted by R^I , is bounded by the surfaces Γ_1 and Γ_2 and is such that outside of R^I we have homogeneous phases, i.e., in the two subvolumes $W(t) \setminus R^I$, denoted by R_i , we have constant densities ρ_i , $i = 1, 2$. We choose a dividing surface Γ and assume the three surfaces to be parallel. The dividing surface is assumed to be transported with the flow velocity field $\mathbf{u}(x, t)$, $x \in \Gamma = \Gamma(t)$. In the interfacial region R^I we have a *mixture* of the two phases. The density of this mixture (total mass per volume) is denoted by ρ^I . Note that in general this density is *not* constant in R^I . This density function can be naturally extended outside R^I by $\rho^I = \rho_i$ in R_i , $i = 1, 2$.

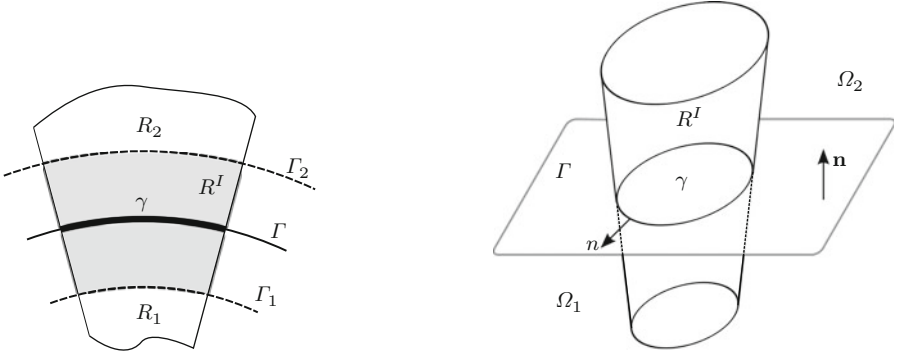


Fig. 1.4. Illustration of cylinder R^I in 2D (left) and 3D (right).

The mass conservation property is modeled by

$$\frac{d}{dt} \int_{W(t)} \rho^I dx = 0. \quad (1.26)$$

Let ρ be the piecewise constant function with constant values ρ_1, ρ_2 in the two subvolumes of $W(t)$ separated by the dividing surface Γ , which are denoted by $W_i(t)$, $i = 1, 2$. From (1.26) we obtain

$$\frac{d}{dt} \left(\int_{W(t)} \rho dx + \int_{R^I} (\rho^I - \rho) dx \right) = 0. \quad (1.27)$$

For a sharp interface model, with a dividing surface Γ and a piecewise constant density ρ , to be a good approximation of the model with an interfacial region and density ρ^I , we introduce a *surface* mass density ρ^Γ . Mass conservation in the sharp interface model then takes the form

$$\frac{d}{dt} \left(\int_{W(t)} \rho dx + \int_{\gamma(t)} \rho^\Gamma ds \right) = 0, \quad (1.28)$$

with $\gamma(t) := \Gamma \cap W(t)$ the part of the dividing surface contained in $W(t)$. Comparing (1.27) with (1.28) we see that we obtain the following relation between ρ^Γ and $\rho^I - \rho$:

$$\int_{\gamma(t)} \rho^\Gamma ds = \int_{R^I} (\rho^I - \rho) dx. \quad (1.29)$$

To elaborate this further we assume that the shape of the material volume is such that the line segment $\partial R^I \cap \partial W(t)$ in Fig. 1.4 (a manifold in the 3D case) is orthogonal to Γ . Then we have (for the 3D case)

$$\int_{R^I} (\rho^I - \rho) dx = \int_{\gamma(t)} \int_{\lambda_-}^{\lambda_+} (\rho^I - \rho)(1 - \kappa_1 \lambda)(1 - \kappa_2 \lambda) d\lambda ds,$$

where λ is the signed distance to the dividing surface Γ . The thickness $\lambda_+ - \lambda_-$ of the local region R^I can be assumed to be very small, and therefore it is reasonable to assume $|\kappa_i \lambda| \ll 1$ for $\lambda \in [\lambda_-, \lambda_+]$. This reasoning suggests that we may identify

$$\rho^\Gamma = \int_{\lambda_-}^{\lambda_+} (\rho^I - \rho) d\lambda, \quad (1.30)$$

which shows that the surface mass density ρ^Γ can be interpreted as an *excess quantity*. Note that ρ^Γ in (1.30) is not necessarily constant or positive on Γ . In the sharp interface model there still is some freedom with respect to the choice of the location of the dividing surface. Different choices imply different excess quantities ρ^Γ . The most popular choice is as follows. For $t = 0$ it is assumed that Γ can be taken such that $\int_{\lambda_-}^{\lambda_+} (\rho^I - \rho) d\lambda = 0$, hence $\rho^\Gamma(x, 0) = 0$ for $x \in \Gamma(0)$. For $t > 0$ the dividing surface is transported by the velocity field \mathbf{u} . From (1.28), Reynolds' transport theorem, the interface transport formula (14.21b) and $\dot{\rho} = 0$ in $W_i(t)$ we obtain

$$\sum_{i=1}^2 \int_{W_i(t)} \rho \operatorname{div} \mathbf{u} dx + \int_{\gamma(t)} \dot{\rho}^\Gamma + \rho^\Gamma \operatorname{div}_\Gamma \mathbf{u} ds = 0.$$

The first term vanishes due to the assumption of incompressibility, i.e. $\operatorname{div} \mathbf{u} = 0$, in $W_i(t)$. Note that in general $\operatorname{div} \mathbf{u} = 0$ in $W_i(t)$ does not imply $\operatorname{div}_\Gamma \mathbf{u} = 0$. For the excess mass density ρ^Γ we thus obtain the equation

$$\dot{\rho}^\Gamma + \rho^\Gamma \operatorname{div}_\Gamma \mathbf{u} = 0 \quad \text{on } \Gamma = \Gamma(t).$$

This equation and the initial condition $\rho^\Gamma(x, 0) = 0$ are fulfilled if we take $\rho^\Gamma \equiv 0$. This derivation motivates the so-called *clean interface assumption*: in the sharp interface model the excess mass density corresponding to the dividing surface is equal to zero. Then the mass conservation equation (1.28) can be simplified to $\frac{d}{dt} \int_{W(t)} \rho dx = 0$, which is consistent with the continuity equations $\operatorname{div} \mathbf{u} = 0$ in Ω_i , which are used in the sharp interface model (1.19). This clean interface assumption is a standard one in sharp interface models without tensesides.

Surface tension as a contact force

In (1.16) we introduced surface tension as a force acting in a direction orthogonal to the (sharp) interface Γ . This orthogonality property holds only if we assume that the surface tension coefficient τ is *constant*, cf. Remark 1.1.3. We summarize some basic facts related to surface tension and from that derive the forces given in (1.16) and (1.22).

Surface tension is an excess force resulting from the fact that on both sides of Γ there are different phases with different molecular forces. Consider a two-phase system in equilibrium, with an interface Γ . Let γ be a (small) connected subset of Γ with boundary $\partial\gamma$ and a normal, denoted by n , which is orthogonal to $\partial\gamma$ and tangential to Γ , cf. Fig. 1.3. Surface tension is defined as a *force per unit of length on $\partial\gamma$ in the direction n* .

This surface tension force is given by $F_s = \tau n$, with τ the *surface tension coefficient*. Note that τ is the magnitude of the surface tension force. The SI unit of τ is Newton per meter. From this definition of F_s it follows that the surface tension force is a *contact force* within the interface Γ . Note, however, that this force is not an intrinsic property of Γ but induced by the two phases on both sides of Γ .

Remark 1.1.4 An equivalent definition of surface tension can be given in terms of energy. Considering the different molecular forces in the two phases it follows that the creation of more interface area is energetically costly and thus the two-phase system will try to (locally) minimize interface area. The amount of work needed to (locally) increase an interface area by an amount δA is given by $\tau \delta A$, with the same surface tension coefficient τ as in the definition used above. In this characterization the surface tension coefficient measures energy per unit of area and the SI unit is joule per square meter.

Let W be a fluid volume which is intersected by the interface Γ and define the interface segment $\gamma = W \cap \Gamma$. Surface tension exerts a *contact force* F_s on $\partial\gamma$. Using the partial integration rule (14.18) the total contact force F_s on $\partial\gamma$ can be rewritten as a force on Γ :

$$\int_{\partial\gamma} \tau n \, d\tilde{s} = - \int_{\gamma} \tau \kappa \mathbf{n} \, ds + \int_{\gamma} \nabla_{\Gamma} \tau \, ds. \quad (1.31)$$

Thus for the case of a constant surface tension coefficient τ we obtain the force as in (1.16) and for the general case the one in (1.22).

Remark 1.1.5 Using the surface tension force representation $F_s = \tau n$ introduced above we derive the classical *Laplace-Young law*, which for a two-phase system in equilibrium and with a spherical interface relates the pressure difference to the mean curvature. We consider a ball with center at the origin and radius R , the boundary of which is the interface of a two-phase system at equilibrium. The constant pressures within and outside the ball are given by p_1 and p_2 , respectively. Note that $[p] = p_1 - p_2 > 0$. We use spherical coordinates:

$$(x_1, x_2, x_3) = r(\sin \theta \cos \phi, \sin \theta \sin \phi, \cos \theta), \quad r \geq 0, \quad \theta \in [0, \pi], \quad \phi \in [0, 2\pi).$$

We consider the upper half of the interface, i.e. the hemisphere given by $S = \{ (r, \theta, \phi) : r = R, \theta \in [0, \frac{1}{2}\pi], \phi \in [0, 2\pi) \}$. There are (only) two forces exerted on S , namely a pressure difference force acting at each point of S and a surface tension force on ∂S . The former is in normal direction and has size $[p]$, the latter has direction $(0, 0, -1)^T$ and size τ , cf. Fig. 1.5. The x_3 -component of the pressure force is given by $\cos \theta [p]$. The resulting total force in x_3 direction must be equal to zero, i.e.

$$2\pi R\tau = [p] \int_S \cos \theta \, ds = [p] \int_0^{2\pi} \int_0^{\frac{1}{2}\pi} \cos \theta \sin \theta R^2 \, d\theta d\phi = [p]\pi R^2$$

must hold. From this we obtain the Laplace-Young law $[p] = \frac{2\tau}{R} = \tau\kappa$, with $\kappa = \frac{2}{R}$ the mean curvature of the sphere with radius R .

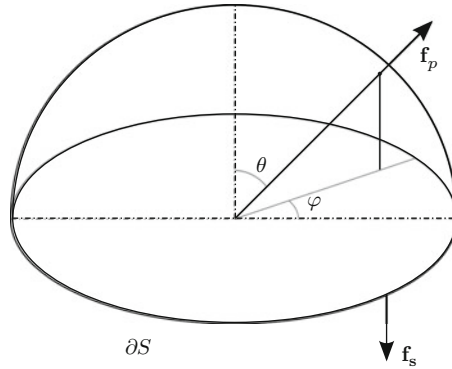


Fig. 1.5. Pressure force \mathbf{f}_p and surface tension force \mathbf{f}_s .

Variable surface tension coefficient: Langmuir model

It is generally accepted and experimentally verified that in many two-phase systems a surfactant changes the properties of the interface and through this can have a significant impact on the fluid dynamics of the system. One very important effect is that a surfactant can cause a change of the surface tension forces. In a system with a clean interface the surface tension coefficient τ is usually assumed to be constant, whereas in a system with surfactants the surface tension coefficient is often considered to be dependent on the local concentration of the surfactant, i.e. $\tau = \tau(S)$. A relatively simple and very popular model for $\tau(S)$ is due to Langmuir (also called Langmuir-Szyszkowski model in the literature). We briefly address the main ideas underlying this model. Consider a system consisting of one bulk phase and its surface Γ . In

the bulk phase a component is dissolved which is adsorbed at the surface. We assume that there is no fluid dynamics and that at a given surface point $x \in \Gamma$ the surface surfactant concentration is locally constant. This surface concentration is denoted by $S(t) = S(x, t)$. Also the bulk concentration of the dissolved component is assumed to be locally constant, and is denoted by $S_b(t) = S_b(x, t)$. There is a maximal surface coverage denoted by S_∞ . A very simple model for describing the ad- and desorption is given by

$$\frac{dS}{dt} = k_{\text{ad}} S_b(t) \left(1 - \frac{S(t)}{S_\infty}\right) - k_{\text{des}} \frac{S(t)}{S_\infty},$$

with positive constants k_{ad} , k_{des} . In equilibrium we have $\frac{dS}{dt} = 0$. Let $S_e = \lim_{t \rightarrow \infty} S_b(t)$ be the equilibrium local bulk concentration. For the equilibrium local surface concentration, denoted by S , we obtain $S = \frac{k_{\text{ad}}}{k_{\text{des}}} S_e (S_\infty - S)$ and thus

$$S = S_\infty \frac{S_e}{k_q + S_e}, \quad \text{with } k_q := \frac{k_{\text{des}}}{k_{\text{ad}}}. \quad (1.32)$$

Hence we have a simple relation between the equilibrium states S (on Γ) and S_e (in the bulk phase). A relation between S , S_e and the surface tension energy τ is obtained from the Gibbs adsorption equation (or Gibbs isotherm), which is often used to relate the changes in concentration of a component in contact with a surface with changes in the surface tension. For $S \gg S_e$, which is the case for most surfactants, and assuming a constant temperature T , this Gibbs adsorption equation is given by

$$\frac{d\tau}{d \ln S_e} = -RTS,$$

with R the gas constant. Using $d \ln S_e = S_e^{-1} dS_e$ and the result in (1.32) we obtain

$$\frac{d\tau}{dS_e} = \frac{-RTS_\infty}{k_q + S_e},$$

and thus

$$\tau = \tau_0 - RTS_\infty \ln(1 + S_e/k_q).$$

From (1.32) we get $1 + S_e/k_q = (1 - S/S_\infty)^{-1}$ and thus we get the following relation between the surface tension coefficient τ and the surfactant concentration S :

$$\tau = \tau_0 + RTS_\infty \ln(1 - S/S_\infty), \quad (1.33)$$

which is the Langmuir model. Here τ_0 is the constant surface tension coefficient for the system with a clean interface. Note that $\tau = \tau(S)$ is a decreasing function of S , i.e., surface tension decreases if the concentration of the surfactant increases. In a realistic two-phase flow system with surfactant the concentration S will *not* be constant on the interface and based on this model one obtains a varying surface tension coefficient with a relatively small value

in those parts of the interface where the surfactant concentration is relatively high.

Other models for $\tau = \tau(S)$ are derived in the literature, e.g. the Frumkin isotherm $\tau(S) = \tau_0 + RT S_\infty \left(\ln(1 - S/S_\infty) - K \left(\frac{S}{S_\infty} \right)^2 \right)$, where K is a measure for the interactions among the adsorbed surfactant particles with $K < 0$ ($K > 0$) if there are significant cohesive (repulsive) forces.

Surface viscosity: Boussinesq-Scriven model

If surfactants are present which cause a variable surface tension coefficient $\tau = \tau(S)$ this results in an effective elasticity of the interface. For certain two-phase flow systems, e.g. with suspended (nano)particles that reside on the interface, it is known that significant other effects also occur. Due to new high-tech applications (e.g., particle-stabilized emulsion, new materials) such systems with colloidal particles at liquid interfaces have attracted a strongly growing interest in the past decade. For modeling the rheological properties of such *particle-laden interfaces* one often introduces an *effective surface viscosity*, [168, 170]. The standard mathematical description of this is by means of the so-called *Boussinesq-Scriven model* which we now introduce, cf. also [225, 45, 219]. First we recall that for the bulk fluid, based on the Cauchy stress principle and assuming the Newtonian stress tensor form $\boldsymbol{\sigma} = -p\mathbf{I} + L(\mathbf{D}(\mathbf{u}))$, with a linear operator L , one can derive the stress tensor representation as in (1.10), i.e.,

$$\boldsymbol{\sigma} = -p\mathbf{I} + \lambda \operatorname{div} \mathbf{u} \mathbf{I} + \mu \mathbf{D}(\mathbf{u}). \quad (1.34)$$

The Boussinesq-Scriven model starts from the (rheological) assumption that the interface behaves like a two-dimensional Newtonian fluid. Recall that surface tension can be characterized as a contact force of the form $\int_{\partial\gamma} \tau n \, d\tilde{s}$, cf. (1.31). In analogy with the approach for a Newtonian fluid in the bulk phase, we start from the structural assumption that on each (small) connected surface segment $\gamma \subset \Gamma$, cf. Fig. 1.3, there is a contact force on $\partial\gamma$ of the form

$$\boldsymbol{\sigma}_\Gamma n, \quad \text{with } \boldsymbol{\sigma}_\Gamma = \tau \mathbf{P} + L(\mathbf{D}_\Gamma(\mathbf{u})), \quad \mathbf{D}_\Gamma(\mathbf{u}) := \mathbf{P}(\nabla_\Gamma \mathbf{u} + (\nabla_\Gamma \mathbf{u})^T) \mathbf{P},$$

with L a linear operator. Recall that $\mathbf{P} = \mathbf{I} - \mathbf{n}\mathbf{n}^T$ is the orthogonal projection onto Γ . This projection is used, since $\boldsymbol{\sigma}_\Gamma n = \boldsymbol{\sigma}_\Gamma \mathbf{P}n$ should represent only contact forces that are tangential to the surface. Note that for $L = 0$ this contact force reduces to the surface tension contact force $\boldsymbol{\sigma}_\Gamma n = \tau \mathbf{P}n = \tau n$. Using the same principles (isotropy, independence of the frame of reference) as in the derivation of (1.34) it can be shown, cf. [225, 15], that the interface stress tensor $\boldsymbol{\sigma}_\Gamma$ must have the following form:

$$\boldsymbol{\sigma}_\Gamma = \tau \mathbf{P} + \tilde{\lambda}_\Gamma \operatorname{div}_\Gamma \mathbf{u} \mathbf{P} + \mu_\Gamma \mathbf{D}_\Gamma(\mathbf{u}), \quad (1.35)$$

with parameters $\tilde{\lambda}_\Gamma, \mu_\Gamma$. This is the interface analogon of the bulk stress tensor representation in (1.34). Note that in general $\operatorname{div}_\Gamma \mathbf{u} \neq 0$, even if $\operatorname{div} \mathbf{u} = 0$

holds. In case of viscous behavior of the interface one takes $\mu_\Gamma > 0$. For certain cases one can derive conditions on the parameter $\tilde{\lambda}_\Gamma$, for example $\tilde{\lambda}_\Gamma > -\mu_\Gamma$ ([225] Sect. 4.9.5). Therefore the interface stress tensor is also written in the form

$$\boldsymbol{\sigma}_\Gamma = \tau \mathbf{P} + (\lambda_\Gamma - \mu_\Gamma) \operatorname{div}_\Gamma \mathbf{u} \mathbf{P} + \mu_\Gamma \mathbf{D}_\Gamma(\mathbf{u}), \quad (1.36)$$

and one often assumes $\lambda_\Gamma = \tilde{\lambda}_\Gamma + \mu_\Gamma > 0$. The parameters μ_Γ and λ_Γ , which we assume to be constants, are referred to as the *interface shear viscosity* and *interface dilatational viscosity*, respectively. In the momentum balance we need the interface force as a force on the interface segment γ . Using the formula $\int_\gamma \operatorname{div}_\Gamma \mathbf{G} \mathbf{P} \, ds = \int_{\partial\gamma} \mathbf{G} \mathbf{n} \, d\tilde{s}$, cf. (14.19), we obtain from (1.36) the interfacial force

$$\begin{aligned} F_3 &= \int_{\partial\gamma} \boldsymbol{\sigma}_\Gamma \mathbf{n} \, d\tilde{s} \\ &= \int_\gamma \operatorname{div}_\Gamma (\tau \mathbf{P}) + (\lambda_\Gamma - \mu_\Gamma) \operatorname{div}_\Gamma (\operatorname{div}_\Gamma \mathbf{u} \mathbf{P}) + \mu_\Gamma \operatorname{div}_\Gamma (\mathbf{D}_\Gamma(\mathbf{u})) \, ds. \end{aligned}$$

Using this interface force F_3 and following the derivation in Sect. 1.1.2 we obtain a generalization of the interface condition in (1.20):

$$[\boldsymbol{\sigma} \mathbf{n}_\Gamma] = \operatorname{div}_\Gamma (\tau \mathbf{P}) + (\lambda_\Gamma - \mu_\Gamma) \operatorname{div}_\Gamma (\operatorname{div}_\Gamma \mathbf{u} \mathbf{P}) + \mu_\Gamma \operatorname{div}_\Gamma (\mathbf{D}_\Gamma(\mathbf{u})) \quad (1.37)$$

on Γ . This is the Boussinesq-Scriven model. For $\lambda_\Gamma = \mu_\Gamma = 0$ this model reduces to the one in (1.23) (or (1.20), if τ is constant) since

$$\operatorname{div}_\Gamma (\tau \mathbf{P}) = \tau \operatorname{div}_\Gamma \mathbf{P} + \nabla_\Gamma \tau = -\tau \kappa \mathbf{n} + \nabla_\Gamma \tau,$$

cf. (14.10). The generalized formulation (1.37) is used to model viscous effects in the interface.

1.2 Initial and boundary conditions

In this section we describe initial and boundary conditions that can be used in the models 1)-4) to make the problem well-posed.

For the NS1 model one needs suitable initial and boundary conditions only for the velocity \mathbf{u} . The initial condition is $\mathbf{u}(x, 0) = \mathbf{u}_0(x)$ with a given function \mathbf{u}_0 , which usually comes from the underlying physical problem. For the boundary conditions we distinguish between *essential* and *natural* boundary conditions. Let $\partial\Omega$ be subdivided into two parts $\partial\Omega = \partial\Omega_D \cup \partial\Omega_N$ with $\partial\Omega_D \cap \partial\Omega_N = \emptyset$. We use essential boundary conditions on $\partial\Omega_D$ that are of Dirichlet type. In applications these describe inflow conditions or conditions at walls (e.g., no-slip). Such Dirichlet conditions are of the form $\mathbf{u}(x, t) = \mathbf{u}_D(x, t)$ for $x \in \partial\Omega_D$, with a given function \mathbf{u}_D . If, for example, $\partial\Omega_D$ corresponds to a fixed wall, then a no-slip boundary condition is

given by $\mathbf{u}(x, t) = 0$ for $x \in \partial\Omega_D$. On $\partial\Omega_N$ we prescribe natural boundary conditions, which are often used to describe outflow conditions. These natural boundary conditions are of the form

$$\boldsymbol{\sigma}\mathbf{n}_\Omega = -p_{ext}\mathbf{n}_\Omega, \quad \text{on } \partial\Omega_N, \quad (1.38)$$

with \mathbf{n}_Ω the outward pointing normal on $\partial\Omega_N$ and p_{ext} a given function (external pressure). For the case $p_{ext} = 0$ we thus obtain a homogeneous natural boundary condition.

Similar initial and boundary conditions can be used for the two-phase flow model NS2. In addition we then need the initial configuration, i.e., $\Gamma(0)$ must be given.

In the model NS2+T in (1.24) one needs in addition initial and boundary conditions for the concentration c . The initial condition is $c(x, 0) = c_0(x)$ with a given initial concentration c_0 . For the boundary conditions the standard ones, namely a Dirichlet (i.e., c given on part of $\partial\Omega$) and a Neumann ($\frac{\partial c}{\partial \mathbf{n}_\Omega}$ given on part of the boundary) condition can be used.

In model NS2+S in (1.25) one has to prescribe an initial concentration $S(x, 0) = S_0(x)$, $x \in \Gamma$, for the surfactant. If Γ is a surface without boundary (droplet) no boundary conditions for S are needed.

1.3 Examples of two-phase flow simulations

In this section we give some simulation results for a two-phase system with a single droplet rising due to buoyancy forces where at the same time transport of some surface active agent (surfactant) on the interface is taking place. This application example is meant to give the reader a first impression of some features of two-phase flow systems and the challenges one is facing when treating such flows numerically.

Before giving details on this numerical simulation, we briefly address the importance of two-phase systems in chemical engineering. One example of such a system is a falling film which is used for cooling by heat transfer from a thin liquid layer to the gaseous phase (liquid-gas system). Another example is an extraction column where mass transport takes place between liquid bubbles and a surrounding liquid (liquid-liquid system). For the design of such bubble column reactors it is desirable to have a model that gives a detailed description of the transport phenomena between the bubbles and the surrounding fluid. Rather than considering the whole column reactor with swarms of bubbles, in a first step only a single droplet is investigated. Even for this simplified case the transport mechanisms are not well understood up to now. One interesting and important phenomenon is the formation of a so-called *stagnant cap* in the downstream part of the droplet. In this stagnant cap region the velocity is much smaller than in the region where the vortices occur, cf. Fig. 1.6. The formation of such stagnant caps has been observed in experiments. In Fig. 1.7

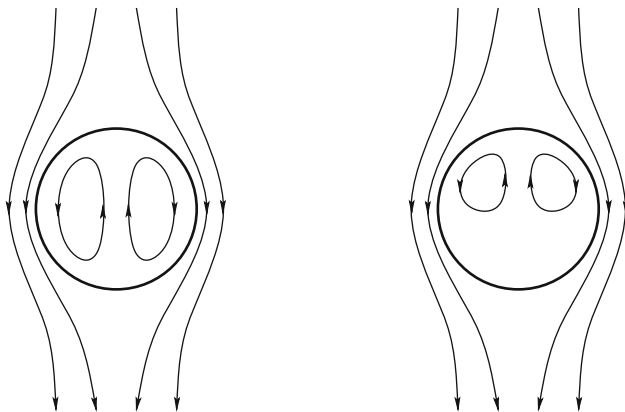


Fig. 1.6. Sketch of flow pattern inside and outside single droplet without (left) and with (right) stagnant cap.

a velocity distribution in a cross-section of a levitated toluene droplet is shown, measured by a fast nuclear magnetic resonance (NMR) technique (from [11]).

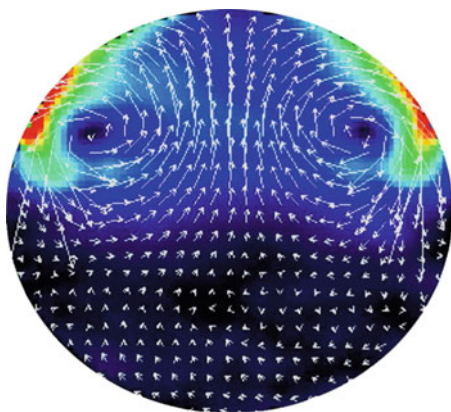


Fig. 1.7. NMR image of measured velocity field in toluene droplet.

There is (experimental) evidence that such regions with very low velocity are caused by surface active substances (surfactants) which adhere to the interface and due to the surrounding flow pattern are transported to the downstream part of the droplet. An interesting (modeling) question in this context is how this surfactant concentration affects the surface tension coefficient, i. e., to find an adequate model for $\tau = \tau(S)$. Furthermore one would like to understand how the variable surface tension coefficient $\tau(S)$ influences the velocity inside the droplet, in particular whether it induces a stagnant cap. It is very hard (for most systems even impossible) to measure in an experiment the

surfactant concentration on the interface or to determine the values of the variable surface tension coefficient. Hence, numerical simulations like the one presented here play a key role for providing more insight.

1.3.1 Numerical simulation of a rising droplet

We present results of a numerical experiment with a single n-butanol droplet inside a rectangular tank $\Omega = [0, 12 \cdot 10^{-3}] \times [0, 30 \cdot 10^{-3}] \times [0, 12 \cdot 10^{-3}] m^3$ filled with water, cf. Fig. 1.8. The material properties of this two-phase system are given in Table 1.1. Initially at rest ($\mathbf{u}_0 = 0 m/s$) the bubble starts to rise in y -direction due to buoyancy effects, with $y = x_2$ and $x = (x_1, x_2, x_3)$.

quantity (unit)	n-butanol	water
$\rho \quad (kg/m^3)$	845.4	986.5
$\mu \quad (kg/m\ s)$	$3.281 \cdot 10^{-3}$	$1.388 \cdot 10^{-3}$
$\tau \quad (N/m)$	$1.63 \cdot 10^{-3}$	

Table 1.1. Material properties of the system n-butanol/water.

For the initial triangulation \mathcal{T}_0 the domain Ω is subdivided into $4 \times 10 \times 4$ sub-cubes each consisting of 6 tetrahedra. Then the grid is refined four times in the vicinity of the interface Γ . As time evolves the grid is adapted to the moving interface. Figure 1.9 shows the droplet and a part of the adaptive mesh for two different time steps. A movie of this numerical simulation is given on the website [90].

For a butanol droplet with radius $1\ mm$, in Fig. 1.10 the y -coordinate of the droplet's barycenter \bar{x}_d is shown as a function of time, where

$$\bar{x}_d(t) = \text{meas}_3(\Omega_1(t))^{-1} \int_{\Omega_1(t)} x \, dx.$$

The average velocity $\bar{\mathbf{u}}_d(t)$ of the drop is given by

$$\bar{\mathbf{u}}_d(t) = \text{meas}_3(\Omega_1(t))^{-1} \int_{\Omega_1(t)} \mathbf{u}(x, t) \, dx.$$

Note that $\bar{x}'_d(t) = \bar{\mathbf{u}}_d(t)$ and, due to incompressibility and immiscibility, $\text{meas}_3(\Omega_1(t)) = \text{meas}_3(\Omega_1(0))$. For a butanol droplet with radius $1\ mm$ Fig. 1.11 shows the rise velocity, which is the second coordinate of the average velocity $\bar{\mathbf{u}}_d(t)$. After a certain time the rise velocity becomes almost constant and the bubble reaches a terminal rise velocity denoted by u_r . For the radius $r_d = 1\ mm$ we obtain $u_r = 53\ mm/s$. For technical applications the

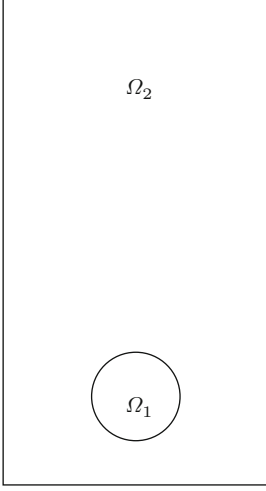


Fig. 1.8. 2D sketch of the rising bubble example.

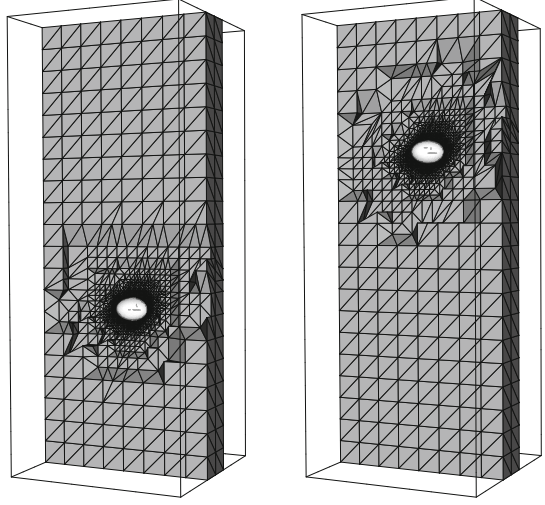


Fig. 1.9. Interface and part of the grid for a rising bubble with radius $r_d = 1$ mm at times $t = 0.2$ s (left) and $t = 0.4$ s (right).

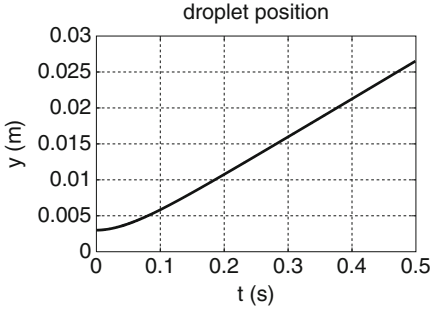


Fig. 1.10. y -coordinate of barycenter of a rising butanol droplet with radius 1 mm as a function of time t .

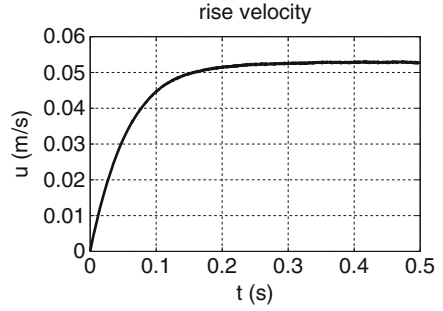


Fig. 1.11. Rise velocity of a butanol droplet with radius 1 mm as a function of time t .

value of the terminal rise velocity is an important quantity, e.g., to predict the duration of a bubble's residence time inside a column reactor.

We computed the terminal rise velocities u_r of rising butanol droplets for different drop radii r_d . For larger droplets with $r_d \geq 1.5$ mm a coarser mesh was used (3 times local refinement instead of 4 times as for the smaller droplets) because of memory limitations. A validation of the simulation results by means of comparison with experimental data is given in [35]. In Fig. 1.12, which is taken from [35], the terminal rise velocity u_r is plotted versus the bubble radius r_d and a comparison of experimental and simulation results is shown. For a discussion of these results we refer to [35].

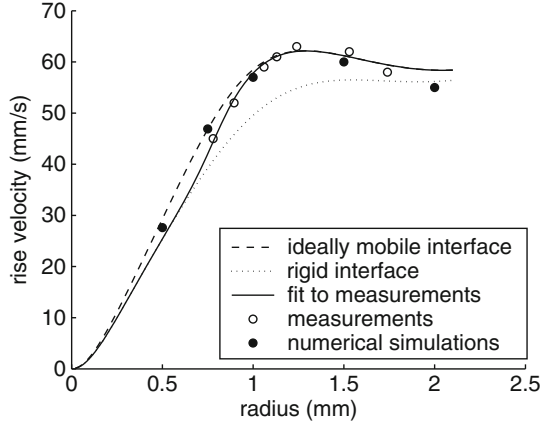


Fig. 1.12. Terminal rise velocities u_r for different droplet radii r_d . Experimental data (open circles), DROPS simulation results (filled circles) and curve fitted to experimental data (solid line).

The droplet shapes of rising butanol droplets for different radii r_d are shown in Fig. 1.13. The droplet shape is almost spherical for $r_d = 0.5 \text{ mm}$ and becomes more and more flattened for larger radii. The corresponding velocity field $\mathbf{u} - \bar{\mathbf{u}}_d$ (which is the velocity with respect to a reference frame moving with droplet speed $\bar{\mathbf{u}}_d$) is visualized on a slice in the middle of the domain. Toroidal vortices can be observed inside the droplets. For $r_d = 2 \text{ mm}$ we also observe a small vortex structure in the wake of the bubble. These numerical results are not able to reproduce a stagnant cap flow pattern as in Fig. 1.6, since the surface tension coefficient τ was assumed to be constant. In the next section we simulate surfactant transport for a rising butanol droplet.

1.3.2 Numerical simulation of a droplet with surfactant transport

We again consider the problem of a rising butanol droplet from the previous section, but now include surfactant transport on Γ . The model NS2+S consists of the two-phase flow problem (1.19)–(1.21) combined with the surfactant transport equation (1.25). The experimental setup and the numerical parameters are chosen as described in Sect. 1.3.1. We take a droplet radius $r_d = 1 \text{ mm}$. The initial constant surfactant concentration is chosen as $S_0 = 1$ and the surfactant diffusion coefficient is set to $D_\Gamma = 10^{-5}$.

As time evolves, the droplet starts to rise and changes its shape. The flow field \mathbf{u} at the interface induces a surfactant transport from the top to the bottom of the droplet. Figure 1.14 shows the droplet's shape and surfactant concentration for $t = 0, 0.1, 0.2, 0.4 \text{ s}$, respectively. The surfactant is collected at the lower part of the droplet while the surfactant concentration at the upper part becomes relatively small. Figure 1.15 shows the surfactant concentration as a function of the vertical coordinate y , with $y = x_2$ and $x = (x_1, x_2, x_3)$,

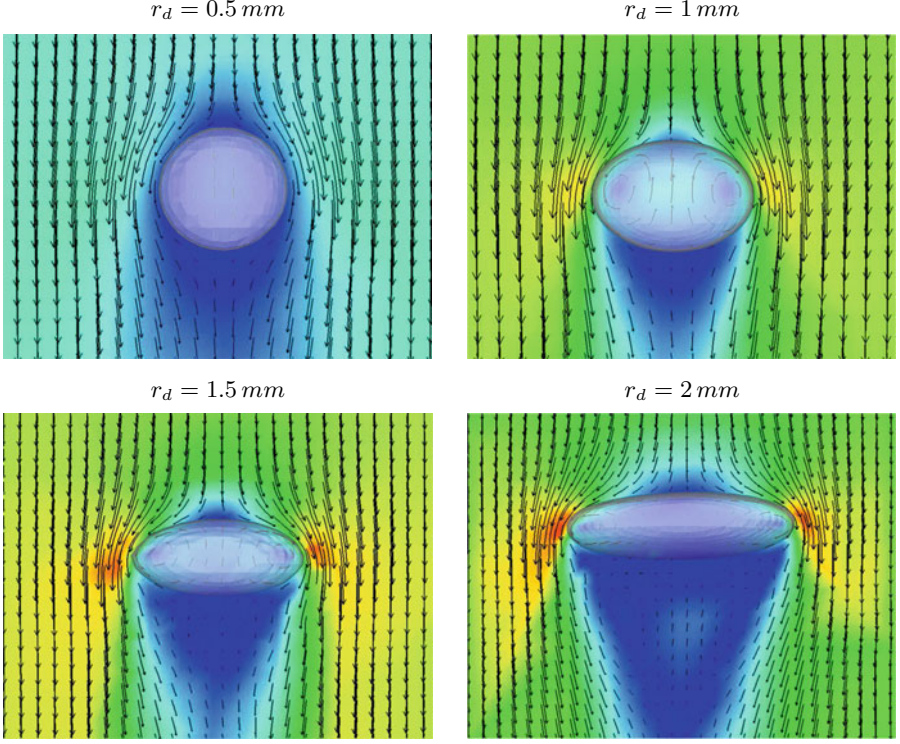


Fig. 1.13. Shape of n-butanol droplets for different radii r_d and velocity field $\mathbf{u} - \bar{\mathbf{u}}_d$ visualized on slice.

for each of the respective times. Hence, each snapshot of the rising droplet in Fig. 1.14 corresponds to one of the graphs in 1.14. For example, the constant surfactant concentration of the initial droplet ($t = 0$ s) is represented in Fig. 1.15 as a straight vertical line of height 2 mm, which corresponds to the initial droplet diameter. The droplet's shape as well as the surfactant profile relative to the droplet becomes almost stationary for $t \geq 0.2$ s, with $S \approx 3.2$ at the bottom and $S \approx 0.015$ at the top of the droplet, i.e., only 1.5% of the initial surfactant concentration.

The next step would be to consider a variable surface tension coefficient τ depending on the surfactant concentration S . At the top of the droplet this would be $\tau \approx 1.63$ mN/m as for the pure n-butanol/water system, while at the bottom the surface tension coefficient would be decreased as an effect of the high surfactant concentration. We do not consider this issue here. In Sect. 11.5.3 we give results of a numerical experiment in which the surface tension coefficient depends on the concentration of a dissolved species close to the interface, i.e. $\tau = \tau(c)$. In that experiment, the variable surface tension induces a stagnant cap as in the right picture in Fig. 1.6.

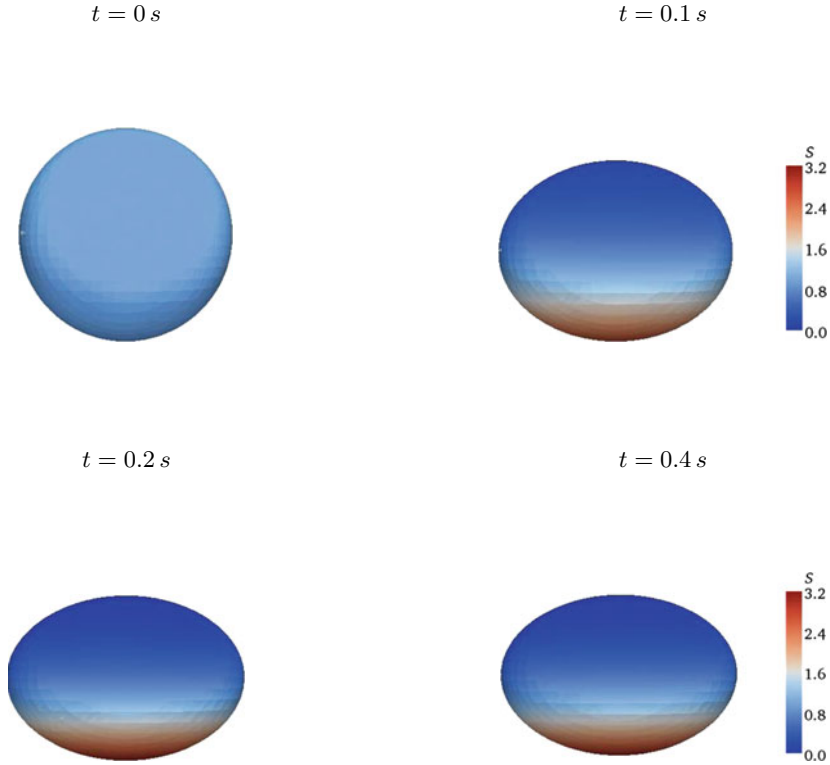


Fig. 1.14. Shape and surfactant concentration S (color-coded) of n-butanol droplet for different time steps $t = 0, 0.1, 0.2, 0.4\text{ s}$.

1.4 Overview of numerical methods

In the following chapters many numerical methods for the simulation of the models introduced in Sect. 1.1 are treated. In this section we give an overview of important methods. for spatial discretization *only finite element methods* will be considered. Besides different finite element methods we also discuss algorithms for the construction of nested multilevel tetrahedral triangulations, implicit time discretization methods and iterative solvers for the resulting discrete problems. We list the main numerical methods:

- A level set method for interface capturing is used. We treat discretization methods for the linear hyperbolic level set equation. Also a fast-marching re-initialization algorithm is discussed.
- The construction of a multilevel hierarchy of nested tetrahedral triangulations is treated. Local refinement and coarsening routines are explained.

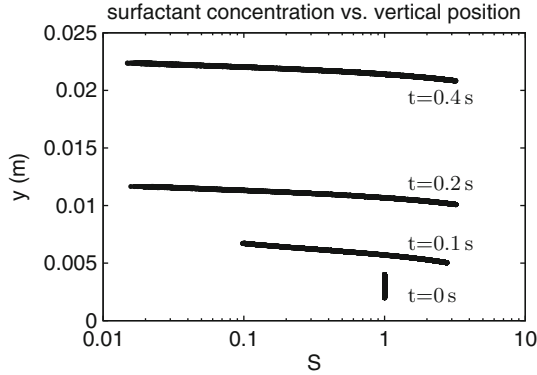


Fig. 1.15. Surfactant concentration S as function of vertical coordinate y for $t = 0, 0.1, 0.2, 0.4$ s, respectively.

- Starting from suitable variational formulations of the models, for spatial discretization we apply finite element techniques based on conforming spaces. Special finite element spaces suitable for functions that are discontinuous across the interface are introduced. We use the XFEM (“extended finite element method”) approach.
- For discretization of the surface tension force a special Laplace-Beltrami method is analyzed.
- For the fluid dynamics problem we derive several implicit time integration methods in which flow variables, surface tension forces and the level set function are strongly coupled.
- After space and time discretization of the fluid dynamics problem one obtains, in each time step, a nonlinear discrete problem in which the flow and level set unknowns are strongly coupled. We analyze an iterative decoupling strategy.
- For the solution of large sparse linear systems preconditioned Krylov subspace methods are discussed. Also inexact Uzawa type solvers for saddle point problems are analyzed. Several Schur complement preconditioners are considered. Multigrid solvers/preconditioners are explained.
- For the discretization of the mass transport equation we consider a method in which the XFEM technique is combined with a so-called Nitsche approach in order to satisfy the Henry interface condition.
- For the discretization of the surfactant convection-diffusion equation on the interface a special Eulerian finite element technique is introduced.
- For the space and time discretization of the mass transport and surfactant transport equations a space-time finite element approach appears to be very natural. We treat such space-time finite element methods.

In Table 1.2 we give a compact overview of all important methods considered, in the form of a matrix of methods. As can be seen from this table, we arrange the different methods according to two criteria, namely *the models for*

which they are used (rows) and the computational method class they belong to (columns). A downward pointing arrow in the table means that methods from the row(s) above are used. To be more specific we briefly address the methods shown in Table 1.2 in a row wise order.

Model NS1 (one-phase Navier-Stokes problem). We explain how a multilevel hierarchy of nested tetrahedral meshes can be constructed, which allows simple local refinement and coarsening algorithms. These *grid related methods* are also used in the numerical simulation of the other models. For spatial discretization we explain the standard Hood-Taylor P_2 - P_1 finite element pair. We briefly address *quadrature rules* to evaluate the integrals that occur in the discrete variational formulation. Spatial discretization results in a large system of nonlinear ordinary differential equations coupled with algebraic constraints (due to $\operatorname{div} \mathbf{u} = 0$), i.e., a DAE system (Differential Algebraic Equation). For this system we discuss several *numerical time integration rules*. A one-step θ -scheme and a fractional-step θ -scheme are treated. Per time step such a time integration rule results in a large nonlinear system of algebraic equations, in which velocity \mathbf{u} and pressure p are coupled. For *linearization* of the term $(\mathbf{u} \cdot \nabla)\mathbf{u}$ a standard Picard iteration (with steplength optimization) is applied. After linearization we have a large sparse linear system of algebraic equations that is of saddle point type. Several efficient *iterative solvers*, like for example preconditioned minimal residual (MINRES), inexact Uzawa and multigrid methods are discussed.

Model NS2 (two-phase Navier-Stokes problem). For the interface representation (“interface capturing”) we use a *level set approach*. In this method one uses a scalar level set function ϕ (which has no physical meaning) whose zero level coincides (approximately, due to discretization errors) with the interface. In the model (1.19)-(1.21) the immiscibility condition in (1.21) is then replaced by a linear hyperbolic partial differential equation for ϕ . An important issue is the *discretization of the level set equation*. For this we use piecewise quadratic finite elements combined with streamline diffusion stabilization (SDFEM). Another topic is the *approximation of the zero level* of this discretization ϕ_h of ϕ ($\Gamma \rightsquigarrow \Gamma_h$). Related to the level set function we also need a *re-initialization method*. We will reformulate the model NS2 such that the interface conditions (1.20) are eliminated and replaced by a *localized force term* (at the interface) in the momentum equation. A main issue is the *discretization of this localized surface tension force*. For this we introduce and analyze a Laplace-Beltrami technique. In this type of problems, due to surface tension, the pressure is discontinuous across the interface. For an appropriate treatment of this discontinuity we introduce a *special extended finite element space* (XFEM). Due to the pressure discontinuity and discontinuities in density and viscosity we need *special quadrature rules*. Application of a time integration rule results in a large nonlinear system of algebraic equations (per time step) in which \mathbf{u} , p and ϕ are coupled. We explain an iterative *decoupling strategy* to split

the coupled problem for \mathbf{u}, p, ϕ into two subproblems for (\mathbf{u}, p) and ϕ , respectively. If in the flow problem there are very large jumps in density and viscosity across the interface (as, for example, in a liquid-gas system) then in order to obtain efficient iterative solvers we propose *special preconditioners* that are robust with respect to variation in the size of these jumps.

Model NS2+T (two-phase flow with mass transport). Due to the Henry interface condition $c_1 = C_H c_2$ (with $C_H \neq 1$) in (1.24), the concentration is discontinuous across the interface. For the spatial discretization of the convection-diffusion equation for the concentration c we use the XFEM technique. In order to satisfy the Henry jump condition at the interface a *technique due to Nitsche* is explained. For the *time integration* we distinguish two cases. If the interface is stationary, a standard method of lines approach can be applied in which the spatial finite element discretization is combined with a θ -scheme for time discretization. In case of a non-stationary interface this approach is not very satisfactory and we treat as alternatives a *Rothe method* (first time, then space) and a *space-time finite element* technique. A simple method for the *decoupling* of (\mathbf{u}, p, ϕ) and c in each time step is discussed.

Model NS2+S (two-phase flow with surfactant transport). In this model we have a convection-diffusion equation on the (evolving) interface Γ , cf. (1.25). For the spatial discretization we use a *special finite element space* that is obtained from suitable restriction of a standard finite element space used for discretization of the flow variables on the tetrahedral triangulation. Again for the time discretization we distinguish between a stationary and a non-stationary interface. For the latter case a *space-time finite element* method is discussed.

The methods addressed above are treated in this monograph and implemented in the DROPS package [90]. We mention a few other research groups in Numerical Analysis and Computational Engineering in which the numerical simulation of two-phase incompressible flow problems is an important research topic: the groups around Bothe [9, 10], Griebel [73], Herrmann [138, 139], Kuipers [80, 88], Lowengrub and Voigt [233, 234], Marchandise [173, 172], Tobiska [115, 118], Tryggvason [243, 182], Weigand [216, 215].

	Grids	spatial discretization	time integration	couplings/linearization	iterative solvers
NS1	↓ multilevel tetrahedral hierarchy; local refinement and coarsening;	Hood-Taylor FE; quadrature;	θ -scheme; fract.-step scheme;	(\mathbf{u}, p) fully coupled; Picard iteration for linearization;	inexact Uzawa; GMRES, GCR, MINRES; Schur compl. precondition.; multigrid method;
		↓ XFEM for p ; P_2 + SDFEM for ϕ ; mass conservation; re-initialization of ϕ ; $\Gamma \rightsquigarrow \Gamma_h$; discretization of $f\Gamma$; special quadrature;	↓ generalized θ -scheme	↓ fixed point for decoupling of $(\mathbf{u}, p) \leftrightarrow \phi$;	↓ special preconditioners (large jumps);
NS2+T	↓	↓ Nitsche approach; XFEM for c ;	↓ Rothe method; space-time FE;	↓ decoupling of $(\mathbf{u}, p, \phi) \leftrightarrow c$;	↓
		↓ Eulerian surface FE method;	↓ space-time FE;	↓ decoupling of $(\mathbf{u}, p, \phi) \leftrightarrow S$;	↓

Table 1.2. Overview of numerical methods.

Numerical Methods for Two-phase Incompressible Flows

Gross, S.; Reusken, A.

2011, XVIII, 482 p., Hardcover

ISBN: 978-3-642-19685-0